

<https://doi.org/10.1038/s41522-025-00660-7>

V-ATPase contributes to the cariogenicity of *Candida albicans*-*Streptococcus mutans* biofilm



Qian Jiang^{1,2,3,8}, Mengmeng Xu^{1,4,8}, Hong Chen^{1,4}, Yao Zhang^{1,4}, Yuting Sun^{1,4}, Li Tao⁵✉, Zheng Wang^{1,4}✉ & Deqin Yang^{1,6,7}✉

The interaction between *Candida albicans* and *Streptococcus mutans* plays an important role in the progression of dental caries. The vacuolar proton pump (V-ATPase) is a vital enzyme regulating the growth and virulence of *C. albicans*, which is a potential target for caries prevention. However, the effect of V-ATPase on the cariogenicity of *C. albicans*-*S. mutans* biofilm remains to be explored. In this study, the detection rate of *C. albicans* in caries-active (group CA) (22.03%) was significantly higher than that in caries-free (group CF) children (8.00%), and the expression of V-ATPase related genes were higher in group CA. Then, the higher expressed V-ATPase coding genes *VMA3*, *VMA4* and *VMA11* in CA group were knocked out. Compared with the wild type SC5314, the mutants showed slower growth rate, inhibited hyphal growth, and defective integrity of cell wall. The biofilm biomass and extracellular polysaccharide (EPS) production of dual biofilm were significantly reduced, and the biofilm structure was impacted. Transcriptome analysis indicated that V-ATPase participated in various metabolisms and biosynthesis pathways of *C. albicans*, and influenced EPS metabolism of *S. mutans*. Finally, compared with the positive control, the caries severity, the biomass and EPS production of dental plaque were significantly reduced after deletion of *VMA3*, *VMA4* and *VMA11* in vivo. This study revealed for the first time the regulating effect of V-ATPase on the cariogenicity of *C. albicans*-*S. mutans* biofilm and its potential mechanisms. The results may provide basis for new strategies of ecological prevention and treatment of dental caries.

Dental caries, a chronic infectious disease occurring in the hard tissue of teeth, has become a major global public health problem because of its high incidence and wide coverage^{1,2}. According to the Global Burden of Disease Study, untreated dental caries in permanent teeth has been the most common disease for the last decade. In 2017, the global prevalence of caries in permanent teeth was 29.4%, affecting up to 2.3 billion people, while caries in deciduous teeth affected 532 million children^{3,4}.

The occurrence and development of dental caries is closely related to the imbalance of dental plaque microbiota. The oral cavity has been considered to possess the second most complex microbiota in human body, only behind the

colon. The oral microbiome is highly diverse, including bacteria, fungi, viruses, archaea and protozoa (eHOMD, <https://homd.org/>), which play important roles in maintaining the homeostasis of oral microenvironment and preventing oral infectious diseases such as dental caries and periodontal disease^{5,6}. Among these microorganisms, *S. mutans* is recognized as the main cariogenic pathogen. Despite its low relative abundance in the oral cavity, it can gain a competitive advantage when the microbial community become unbalanced due to local microenvironmental changes. It can rapidly ferment carbohydrates to produce acid and synthesize intracellular and extracellular polysaccharides, and promote the adhesion and aggregation of

¹Stomatological Hospital of Chongqing Medical University, Chongqing Key Laboratory of Oral Diseases, 404100 Chongqing, China. ²Department of Conservative Dentistry and Endodontics, Shanghai Stomatological Hospital & School of Stomatology, Fudan University, Shanghai, China. ³Department of Stomatology, Beijing Tongren Hospital, Capital Medical University, Beijing, China. ⁴Chongqing Key Laboratory of Oral Diseases and Biomedical Sciences, Chongqing, China.

⁵Department of Infectious Diseases, Huashan Hospital, State Key Laboratory of Genetic Engineering, School of Life Sciences, Fudan University, Shanghai, China.

⁶Shanghai Key Laboratory of Craniomaxillofacial Development and Diseases, Fudan University, Shanghai, China. ⁷Present address: Department of Conservative Dentistry and Endodontics, Shanghai Stomatological Hospital & School of Stomatology, Fudan University, Shanghai, China. ⁸These authors contributed equally:

Qian Jiang, Mengmeng Xu. ✉e-mail: taoli@fudan.edu.cn; wangzheng@hospital.cqmu.edu.cn; 500246@hospital.cqmu.edu.cn; yangdeqin_@fudan.edu.cn

microorganisms on the tooth surface^{7,8}. In recent years, the role of fungi in oral diseases has attracted more and more attention, among which *C. albicans* is the main fungus related to oral diseases. It usually colonized on the surface of oral mucosa as commensal microbe. Some systemic and local factors such as systemic chronic diseases, immunodeficiency, poor oral hygiene, wearing removable dentures or appliances can increase its detection rate^{9–11}. Similar to *S. mutans*, *C. albicans* possesses cariogenic abilities such as adhesion, acid production and resistance, and biofilm formation. It can invade the deep dentine through its hyphae, contributing to the progression of dental caries by cross-kingdom interaction with *S. mutans*.

As common symbiotic microbes in the oral cavity, the interaction of *C. albicans* and *S. mutans* plays an important role in the maturation of dental plaque and the progression of dental caries. The colonization of *C. albicans* reduces the local oxygen level and induces the imbalance of oral microorganisms, making the local environment more suitable for *S. mutans*. It can colonize on the tooth surface through the building block provided by *S. mutans*, and its hyphae promotes its adhesion to other bacteria including *S. mutans*. Then they form a symbiotic biofilm, which help resist against stress from the host and the external environment^{12,13}. In addition, *C. albicans* can enhance the cariogenicity of *S. mutans* by increasing the production of extracellular polysaccharides (EPS) and the expression of virulence genes such as *gtfB* and *fabM*¹⁴. Some animal experiments showed increased incidence and severity of dental caries in rats infected with *C. albicans* and *S. mutans*, compared with those infected with a single one^{15,16}. Clinical studies have also shown that the detection rates of *C. albicans* in early childhood caries and root caries are significantly increased^{17–19}.

Vacuole is a vital structure for *C. albicans* to adapt to environmental stress and maintain virulence. Vacuolar proton-translocating ATPase (V-ATPase) is the main proton pump on the vacuolar membrane, responsible for pH homeostasis regulation, stress response, and hyphal growth of *C. albicans*²⁰. As shown in Fig. 1, V-ATPase is a rotating multi-subunit protein complex. The V₁ domain located in the cytoplasm is composed of eight subunits of ABCDEFGH, which is responsible for ATP hydrolysis to provide energy for H⁺ transport. The V₀ domain across the membrane is composed of adef subunits and a “c ring” structure, which provides a transport channel²¹. Each subunit of V-ATPase is encoded by a specific gene. The V₁ A and B encoded by *VMA1* and *VMA2* constitute a hexamer and participate in ATP binding and hydrolysis²². The c, c' and c'' encoded by *VMA3*, *VMA11* and *VMA16* constitute the “c ring”, which is the main site of proton transport. By rotating and combining with the two hemichannels of V₀ a, it can transport H⁺ from cytoplasm to vacuole to maintain the cytoplasmic pH homeostasis and the activities of various degradation enzymes in the vacuole²³. The subunits of V₀ d, V₁ D, and V₁ F are encoded by *VMA6*, *VMA7*, and *VMA8*. They constitute the central axis, which rotates with the “c ring” to accomplish proton transport^{24,25}. *VMA4*-encoded V₁ E and *VMA5*-encoded V₁ C play important roles in the connection and stability of

V-ATPase^{26,27}. These encoding genes regulate the assembly of all the subunits to guarantee the integrity of V-ATPase structure and function, and to maintain the survival and virulence of *C. albicans*^{28,29}. Studies have found that inhibition or knockout of these genes in *C. albicans* can lead to abnormal morphology and function of vacuole, hyphal development defects, and reduced adaptability to environment, which is manifested as attenuated or avirulent in mouse models of systemic candidiasis^{22–27}.

In recent years, reducing the cariogenicity of the *C. albicans*-*S. mutans* biofilm by interfering with its interaction has posed a new idea for the prevention and therapy of dental caries^{30,31}. As an important protein in regulating virulence in *C. albicans*, V-ATPase is a potential target for the resistance of *C. albicans*-*S. mutans* biofilm and the treatment of dental caries. However, there is a lack of studies about the regulating effect of V-ATPase on the *C. albicans*-*S. mutans* interaction and the cariogenicity of biofilm.

This study verified the relationship between dental caries and *C. albicans* and its V-ATPase through the isolation of clinical strains of *C. albicans* and detection of gene expressions. On this basis, we constructed V-ATPase related gene knockout mutants for *VMA3* and *VMA4*, which had significantly high expressions in caries groups, as well as *VMA11*, the encoding gene of V₀ c' subunit without homologous protein in human body. The regulating effect of V-ATPase on cariogenicity of *C. albicans*-*S. mutans* biofilm and its mechanisms were elucidated through researches in vitro and in vivo. This study is expected to provide basis for seeking potential targets for early ecological prevention and treatment of dental caries.

Results

C. albicans and V-ATPase were closely related to dental caries in children

As shown in Table 1, 59 caries-active children and 50 caries-free children were enrolled in this study. *C. albicans* was detected in 13 samples of group CA and 4 samples of group CF. The detection rate of *C. albicans* in group CA was 22.03%, significantly higher than that in group CF (8.00%, $p < 0.05$), suggesting that the colonization of *C. albicans* may increase the risk of dental caries in children.

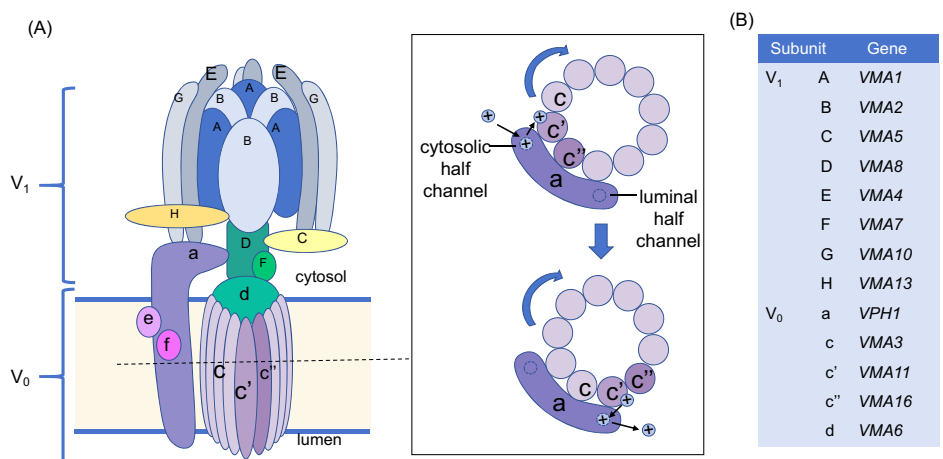
Then we isolated clinical strains of *C. albicans* from caries-active children (Fig. 2A, B), and detected the expression levels of V-ATPase related genes in *C. albicans* clinical strains were detected by qPCR. As shown in Fig. 2C, six genes showed significant differences between the two groups ($P < 0.05$). Among them, the expression of *VMA3*, *VMA4*, *VMA8*, *VMA11*, and *VMA13* were significantly higher in group CA, suggesting that these genes may be involved to the cariogenicity of *C. albicans*.

The growth characteristics of *C. albicans* were regulated by V-ATPase

Based on the results of the gene expressions, we constructed gene knockout mutants for *VMA3* and *VMA4*, which were highly expressed in caries group,

Fig. 1 | The structure and function of V-ATPase.

A The pattern of V-ATPase structure and proton transportation. **B** The encoding genes of each subunit.



as well as *VMA11*, the encoding gene of V_0 c' subunit without homologous protein in human body, to further study the regulating effect of V-ATPase on the growth of *C. albicans* and the cariogenicity of *C. albicans*-*S. mutans* biofilm. The construction of knockout mutants was shown in Fig. S1.

The growth curves of *C. albicans* WT and V-ATPase gene deletion mutants are shown in Fig. 3A. Compared with the WT, the time for the knockout mutants to reach the logarithmic phase and the stable phase was delayed. Among them, the growth curves of *VMA3* and *VMA4* knockout mutants almost overlap, and the growth of *VMA11* knockout mutants was slightly faster. The results showed that the growth of *C. albicans* was inhibited after the knockout of V-ATPase related genes.

Table 1 | Basic information of subjects and detection rate of *C. albicans*

	Caries-active (n = 59)	Caries-free (n = 50)	P value
Age (years)	6.84 ± 2.14	7.59 ± 3.38	0.21
Gender			0.83
Male	26	21	
Female	33	29	
DMFT/dmft	3.91 ± 1.89	0	
Detection of <i>C. albicans</i>	13 (22.03%)	4 (8.00%)	0.04

As shown in Fig. 3B, V-ATPase gene deletion mutants showed growth inhibition on YPD medium, with decreased colony size. And the cells of knockout mutants were flat, with different sizes and unclear outline of organelles. The observation under SEM showed that most cells of the WT were round with smooth surfaces, whereas the cells of *VMA3/VMA4/VMA11* knockout mutants were abnormally shaped, with different sizes and deformities such as cell shrinkage, rupture, and even exfoliation (Fig. 3C), indicating that *VMA3*, *VMA4*, and *VMA11* played an important role in the growth and morphology of *C. albicans*.

The hyphal growth was induced using Spider medium (Fig. 3D). The *VMA3/VMA4/VMA11* knockout mutants showed deficiency in hyphal growth, compared with the WT. Among them, and *VMA3* and *VMA4* knockout mutants showed significantly smaller and smoother colonies. In Spider liquid medium, most cells of the WT could form long and interlaced hyphae, while cells of knockout mutants were all maintained as yeasts, indicating that *VMA3*, *VMA4*, and *VMA11* were involved in the hyphal growth of *C. albicans*.

The growth conditions of *C. albicans* in the medium with different pH values are shown in Fig. 3E. Compared with the WT, the growth of *VMA3*, *VMA4*, and *VMA11* knockout mutants in acidic environment (pH 4 and pH 5) showed no significant differences, but the growth in alkaline environment (pH 7.5 and pH 8) was significantly inhibited, indicating that V-ATPase genes *VMA3*, *VMA4*, and *VMA11* were involved in regulating the alkali resistance of *C. albicans*.

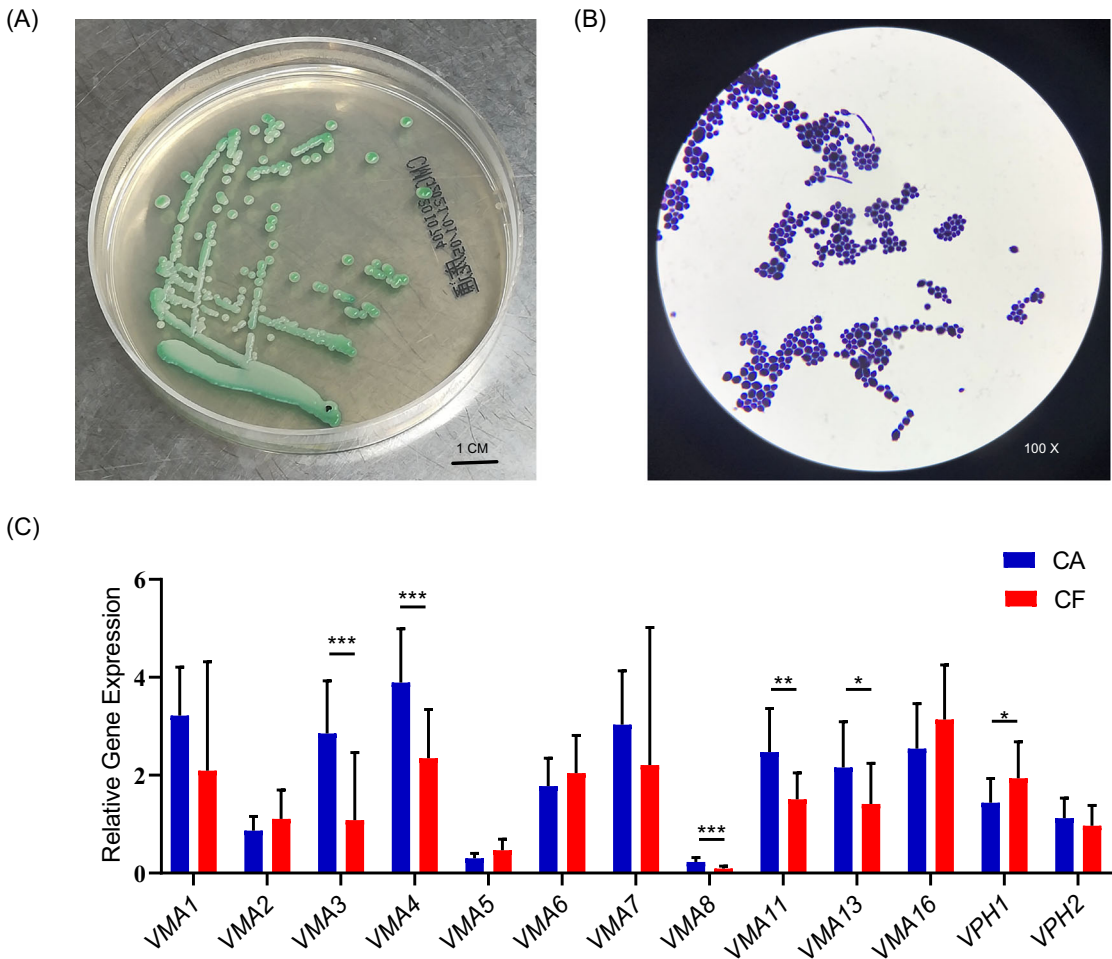


Fig. 2 | *C. albicans* and its V-ATPase are associated with dental caries in children. **A** Colony morphology of clinical *C. albicans* strains on selective medium from caries samples. **B** Cell morphology of clinical *C. albicans* strains after Gram stain. **C** V-ATPase related gene expression of *C. albicans* clinical strains. (* $p < 0.05$, ** $p < 0.01$, *** $p < 0.001$).

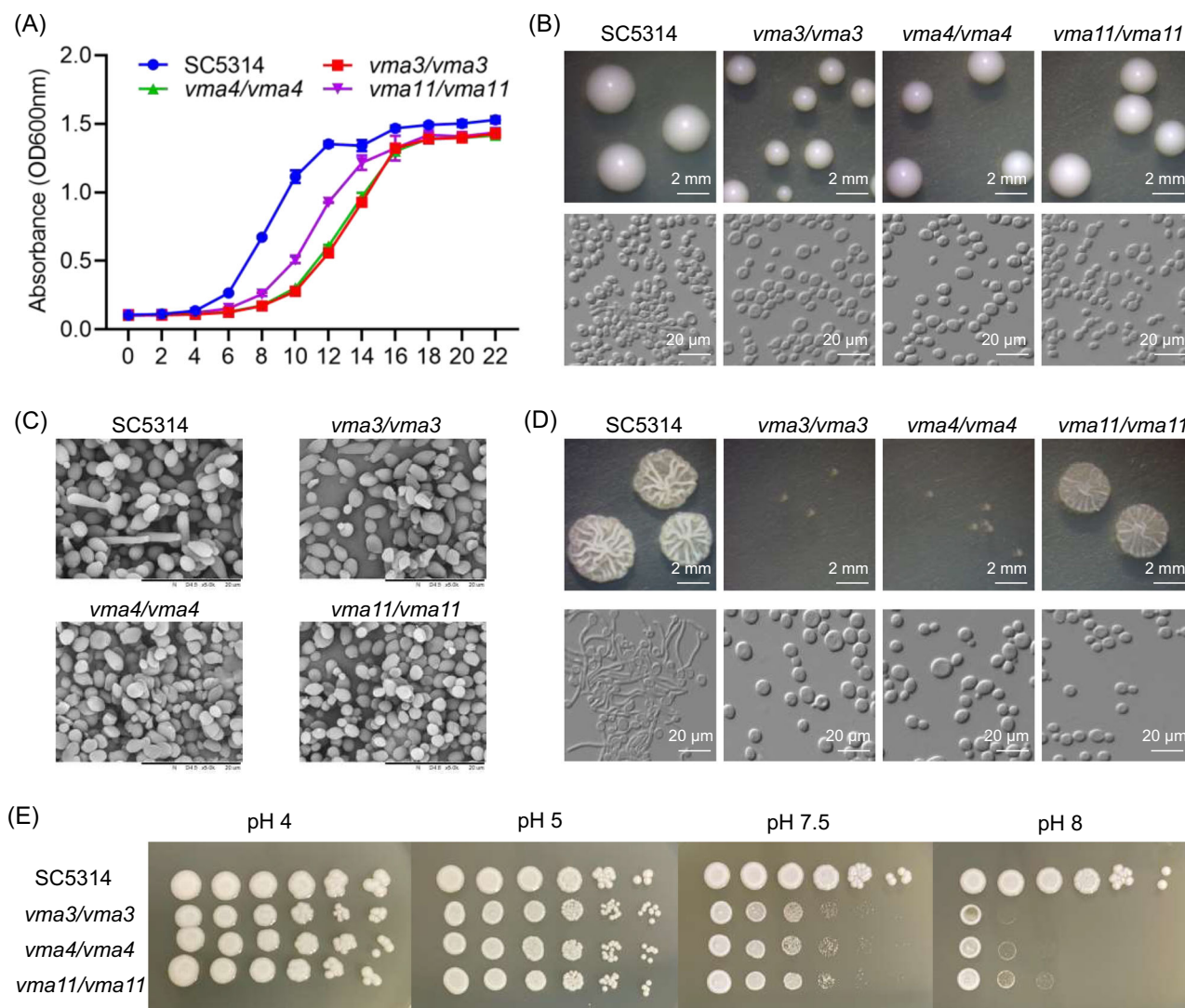


Fig. 3 | V-ATPase gene deletion mutants exhibit different growth phenotype.

A Growth curves of different strains. **B** Morphology of colony and cell incubated on YPD. Green arrow indicates nucleus, red arrow indicates vacuole, and blue arrow

indicates hyphae. **C** Morphology of fungal cells under SEM. Red arrows indicate abnormal shapes. **D** Morphology of colony and cell incubated on Spider. **E** Growth on plates with different pH values.

V-ATPase was involved in the morphology of *C. albicans*-*S. mutans* biofilm

Since V-ATPase affected the growth and morphology of *C. albicans*, we aimed to study the effect of these changes on the *C. albicans*-*S. mutans* dual-species biofilm.

The biofilm biomass was measured by crystal violet assay (Fig. 4A). The *VMA3*, *VMA4*, and *VMA11* knockout mutants showed reduced ability to form both single-species biofilm and dual-species biofilm with *S. mutans* ($P < 0.001$).

The spatial distribution of *C. albicans* and *S. mutans* in the dual-species biofilm was detected by FISH (Fig. 4B). In the *C. albicans* WT-*S. mutans* biofilm, a large number of hyphae formed a network structure and provided a wide range of adhesion sites for *S. mutans*. The dual-species biofilms of *S. mutans* and the *VMA3*, *VMA4* and *VMA11* knockout mutants were loose, with significantly decreased *C. albicans* cells and the proportion of hyphae. Quantitative analysis showed decreased number of *C. albicans* cells in the three gene deletion strains and decreased number of *S. mutans* cells in *VMA3* and *VMA4* deletion strains (Fig. 4C, $P < 0.01$).

In addition, the morphology of biofilm was observed using SEM. As shown in Fig. 4D, compared with the *C. albicans* WT-*S. mutans* biofilm, the mixed biofilms of *S. mutans* and the *VMA3*, *VMA4* and *VMA11* knockout mutants showed loose biofilm structures with decreased proportion of

hyphae, less tight adhesion between the two species, and decreased extracellular matrix.

V-ATPase affected the EPS production of *C. albicans*-*S. mutans* biofilm

The extracellular polysaccharides (EPS) synthesized by *S. mutans* constitute one of the major virulence factors of biofilms. Therefore, we further detected the EPS production and composition of *C. albicans*-*S. mutans* biofilm by anthrone method. The contents of water-soluble glucan (WSG) and water-insoluble glucan (WIG) in dual-species biofilms are demonstrated in Fig. 5A. Compared with the WT, the *VMA3* and *VMA4* knockout mutants showed significantly reduced WSG generation ($P < 0.001$), while no significant difference was found in *VMA11* knockout mutants. All the three gene deletion strains showed decreases in the production of WIG ($P < 0.001$).

To visualize EPS distribution, the structures of *C. albicans*-*S. mutans* biofilm were observed under CLSM. Quantitative analysis showed significantly decreased biofilm thickness in the dual-species biofilm formed by *S. mutans* and the V-ATPase gene knockout mutants (Fig. 5B, $P < 0.05$). As shown in Fig. 5C, in the dual-species biofilm of *C. albicans* WT-*S. mutans*, microbes aggregated and surrounded within a matrix of EPS, forming a complex and dense biofilm structure. However, the number of microbes and

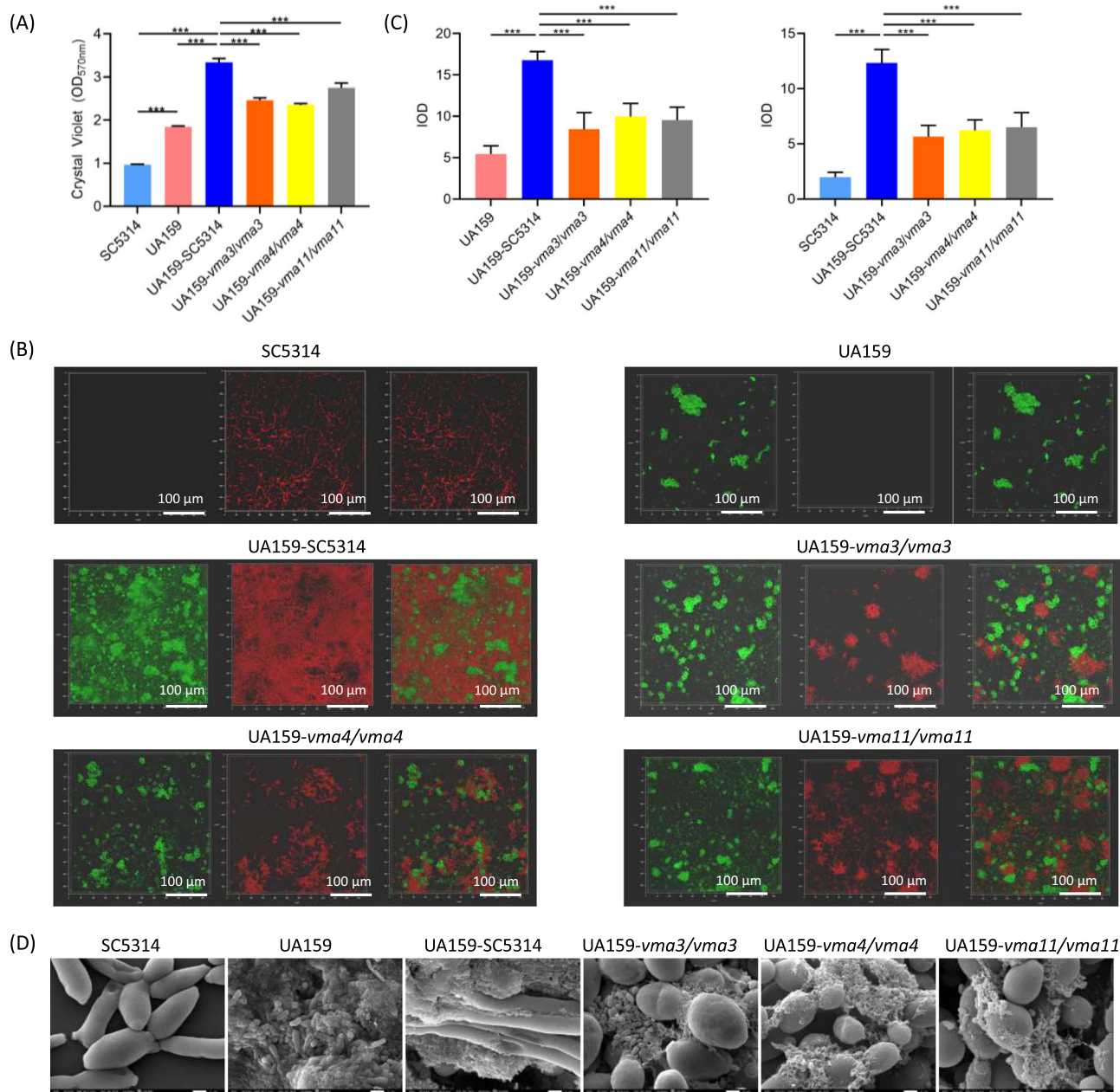


Fig. 4 | V-ATPase genes regulate morphology of *C. albicans*-*S. mutans* biofilm. **A** Biomass of single-species and dual-species biofilm. **B** The structure of biofilm labeled with FISH probes. *S. mutans* was labeled green, *C. albicans* was labeled red.

C Quantitative analysis of *C. albicans* and *S. mutans*. **D** Morphology of *C. albicans*-*S. mutans* biofilm under SEM. The results are based on three independent experiments and represent as mean \pm SD. (***) $p < 0.001$.

the EPS generation decreased in the dual-species biofilm of *S. mutans* and the V-ATPase gene knockout mutants, manifesting as scattered blocks and loose biofilm structures.

To explain the reason for the EPS decrease, we detected the gene expressions of *S. mutans* by qPCR. As shown in Fig. 5D, the expression levels of EPS synthesis-related genes *gtfB/gtfC/gtfD* and adhesion-related genes *gbpB/gbpC* decreased after co-culture with *VMA3/VMA4/VMA11* knockout mutants, while the expression of EPS decomposition genes *dexA* and *dexB* were significantly up-regulated ($P < 0.01$).

V-ATPase regulated the gene expressions of *C. albicans* in dual-species biofilm

Transcriptome sequencing of *C. albicans* in dual-species biofilm detected 5849, 5959, 5966, and 5920 genes in the WT and *VMA3/VMA4/VMA11* knockout mutants respectively, of which 5795 genes were

common in the four groups (Fig. 6A). Principal component analysis (PCA) showed that gene expression in the *VMA3* and *VMA4* knockout groups was generally similar, separated from neither the WT nor *VMA11* knockout group (Fig. 6B). Compared with the WT, 1339 (787 up-regulated, 552 down regulated), 1199 (692 up-regulated, 507 down regulated), and 548 (248 up-regulated, 300 down regulated) differentially expressed genes were detected in the *VMA3*, *VMA4*, and *VMA11* knockouts respectively (Fig. 6C). According to KEGG pathway annotation and enrichment analysis, the up-regulated genes were mainly involved in meiosis, while the down-regulated genes were mainly involved in pyruvate and amino acid metabolism, ribosome, and biosynthesis of cofactors (Fig. 6D). Consistently, we also verified the hyphal formation and adhere related genes by RT-qPCR, and the results showed that the expression of *Als1*, *Als3*, *Als5*, *Efg1* and *Ume6* genes in the knockout mutant group was down-regulated (Fig. 6E).

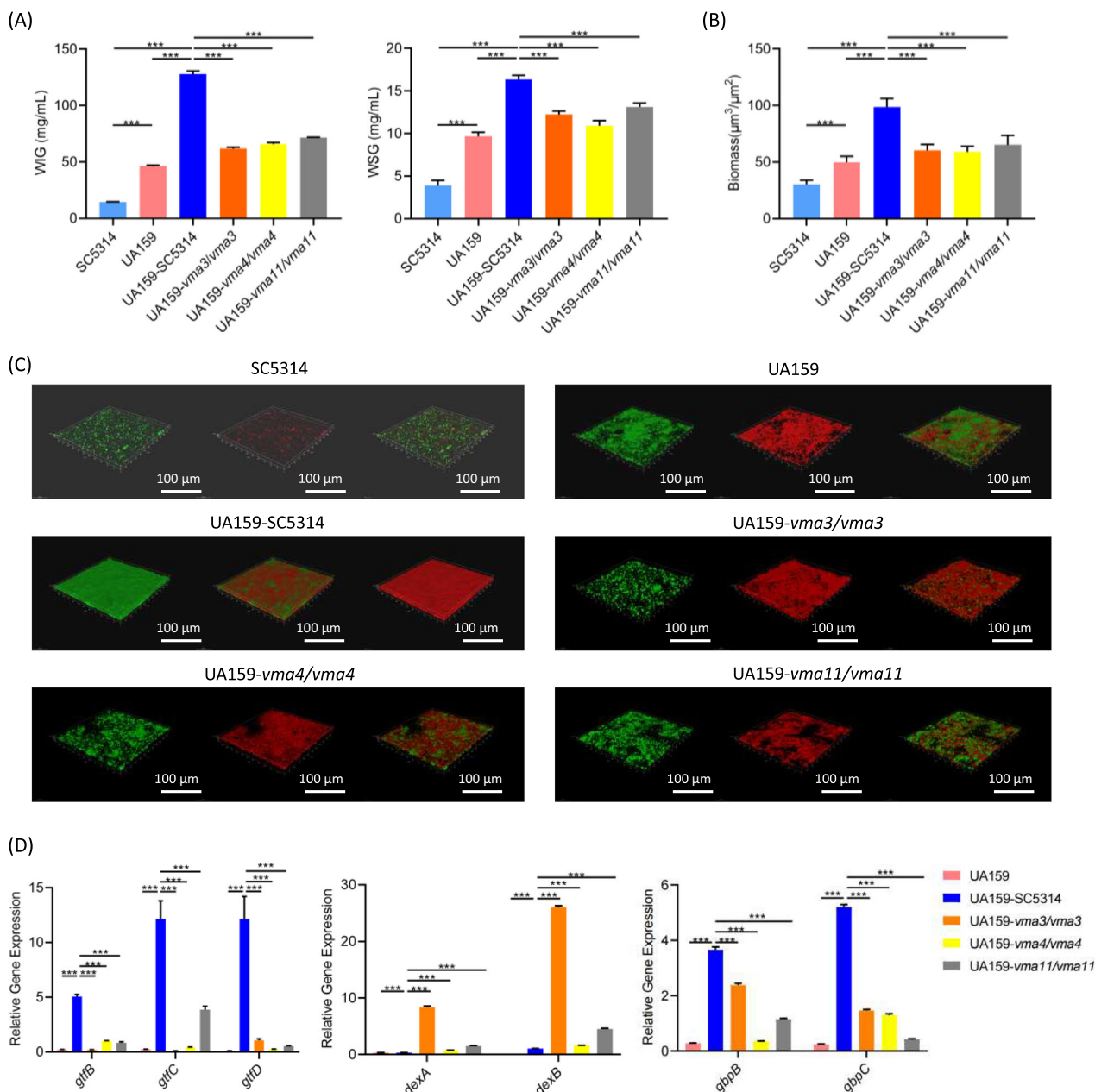


Fig. 5 | V-ATPase genes regulate EPS production of *C. albicans*-*S. mutans* biofilm. **A** EPS generation assessed by anthrone method. The water-soluble (WSG) and water-insoluble (WIG) polysaccharides were measured respectively. **B** The biomass

of biofilm. **C** Biofilm structure under CLSM. *C. albicans* and *S. mutans* were labeled green, EPS was labeled red. **D** Gene expressions of *S. mutans*. The results are based on three independent experiments and represent as mean \pm SD. (***) $p < 0.001$.

The cariogenicity of *C. albicans*-*S. mutans* biofilm was influenced by V-ATPase

To further confirm the effect of V-ATPase on the cariogenicity of *C. albicans*-*S. mutans* biofilm in vivo, the dental caries on the mandibular molars of rats were observed and assessed by Keyes' method (Fig. 7A, B). The blank control and the negative control group showed no smooth surface caries and no more than one pit and fissure caries. Demineralization and shallow caries could be found in the *S. mutans* single-species group and dual-species groups with *C. albicans* VMA3/VMA4/VMA11 knockout mutants. The number and severity of caries lesions in the *S. mutans*-*C. albicans* WT group were higher than those in other groups ($P < 0.05$).

The structures of dental plaque were observed under CLSM and quantitatively analyzed (Fig. 7C, D). In the positive control (*S. mutans*-*C. albicans* WT) group, the dental plaque almost covered the entire tooth surface, with a large number of microbes and EPS. The coverage and thickness of dental plaques and the number of microbes and EPS

significantly decreased in the *S. mutans* single-species group and dual-species groups with gene deletion strains ($P < 0.05$).

The morphology of dental plaque near the gingival margin on the buccal side of the molars was observed under SEM (Fig. 7E). A thick and dense biofilm with a large number of extracellular matrix and hyphae was found on the tooth surface of the *S. mutans*-*C. albicans* WT group. The dental plaque was scattered in the blank control and the negative control group. The thickness and density of dental plaque in the *S. mutans* single-species group and dual-species groups with gene deletion strains were lower than those of the *S. mutans*-*C. albicans* WT group.

Discussion

C. albicans and *S. mutans* are common symbiotic microbes and opportunistic pathogens in the oral cavity. They can affect the oral microbial balance by interacting with each other, playing critical roles in the occurrence and development of dental caries^{32,33}. *C. albicans* can be detected in 30–60%

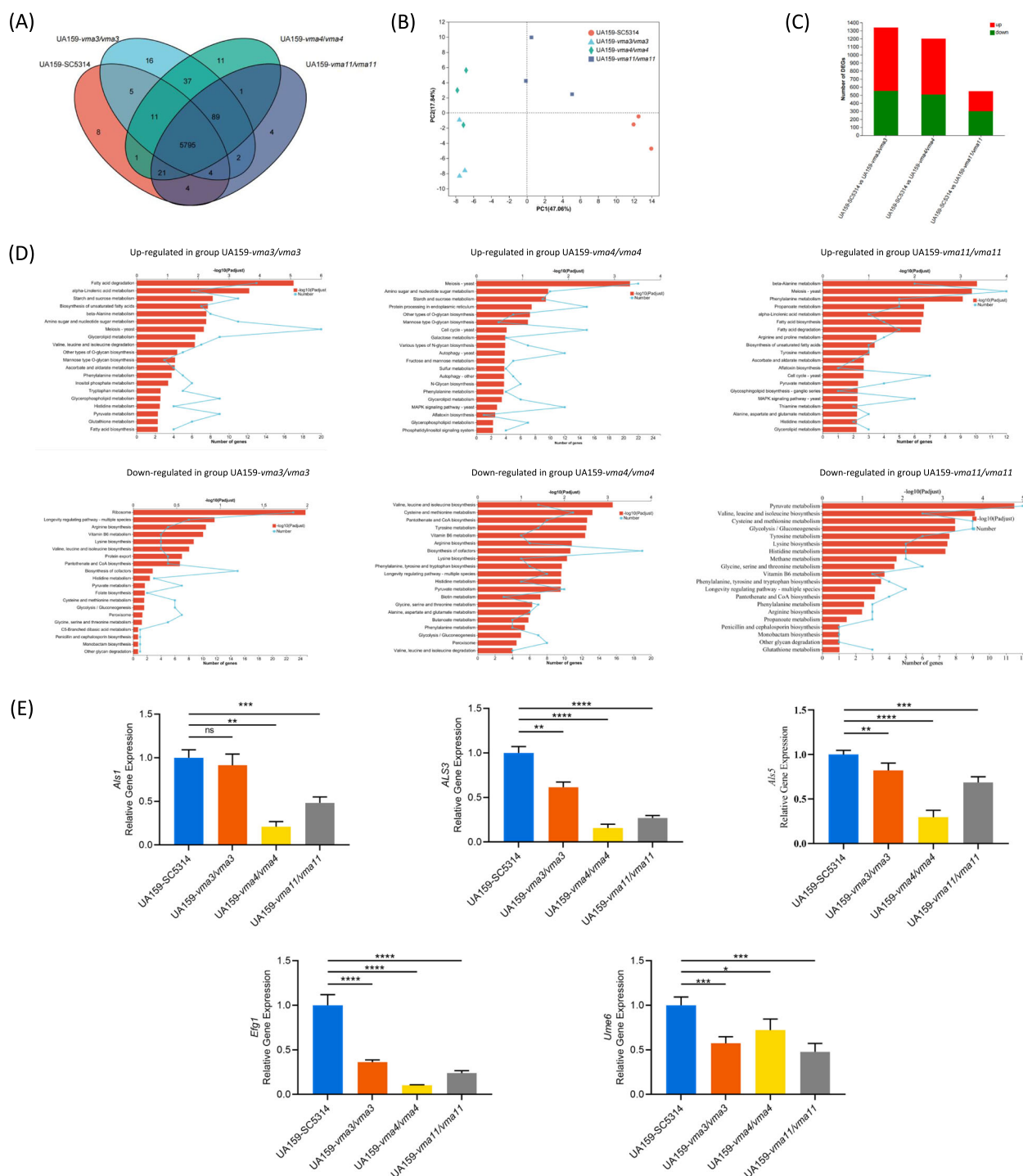


Fig. 6 | Transcriptome analysis of *C. albicans* in dual-species biofilm. A Venn diagram. **B** PCA analysis. **C** Differentially expressed genes. **D** KEGG pathway annotation and enrichment analysis of differentially expressed genes. **E** Hyphal

formation and adhere genes expressions of *C. albicans*. The results are based on three independent experiments and represent as mean \pm SD. (* p < 0.05, ** p < 0.01, *** p < 0.001, **** p < 0.0001, ns, not significant).

peoples' oral cavity, mostly colonized on the mucosal surface¹⁰. In this study, samples were collected from supragingival plaque, the site most closely related with dental caries. Although the detection rate of *C. albicans* was lower than that of oral mucosa and saliva, it was significantly higher in children with dental caries than that in healthy controls. The results confirmed that *C. albicans* was closely related to caries activity in children, thus it should be taken into consideration of early risk assessment of caries in children.

Because of the relationship between *C. albicans* and dental caries, it is of great significance in clinical prevention and treatment to study the

cariogenic mechanism of *C. albicans*. V-ATPase is an important protein of *C. albicans* in environmental stress adaption, hyphal development, and virulence maintenance, which is considered as a potential target for resisting *C. albicans* infection³⁴. This study isolated *C. albicans* from dental plaque of children with different caries conditions and analyzed the expression levels of V-ATPase related genes in the clinical isolates. The results showed that *VMA3*, *VMA4*, *VMA8*, *VMA11*, and *VMA13* may be involved in regulating the cariogenicity of *C. albicans*. Among these genes, *VMA3* and *VMA4* showed the highest expressions and the most significant differences between caries-active and caries-free group, while *VMA11* encoded V_0 c' that has no

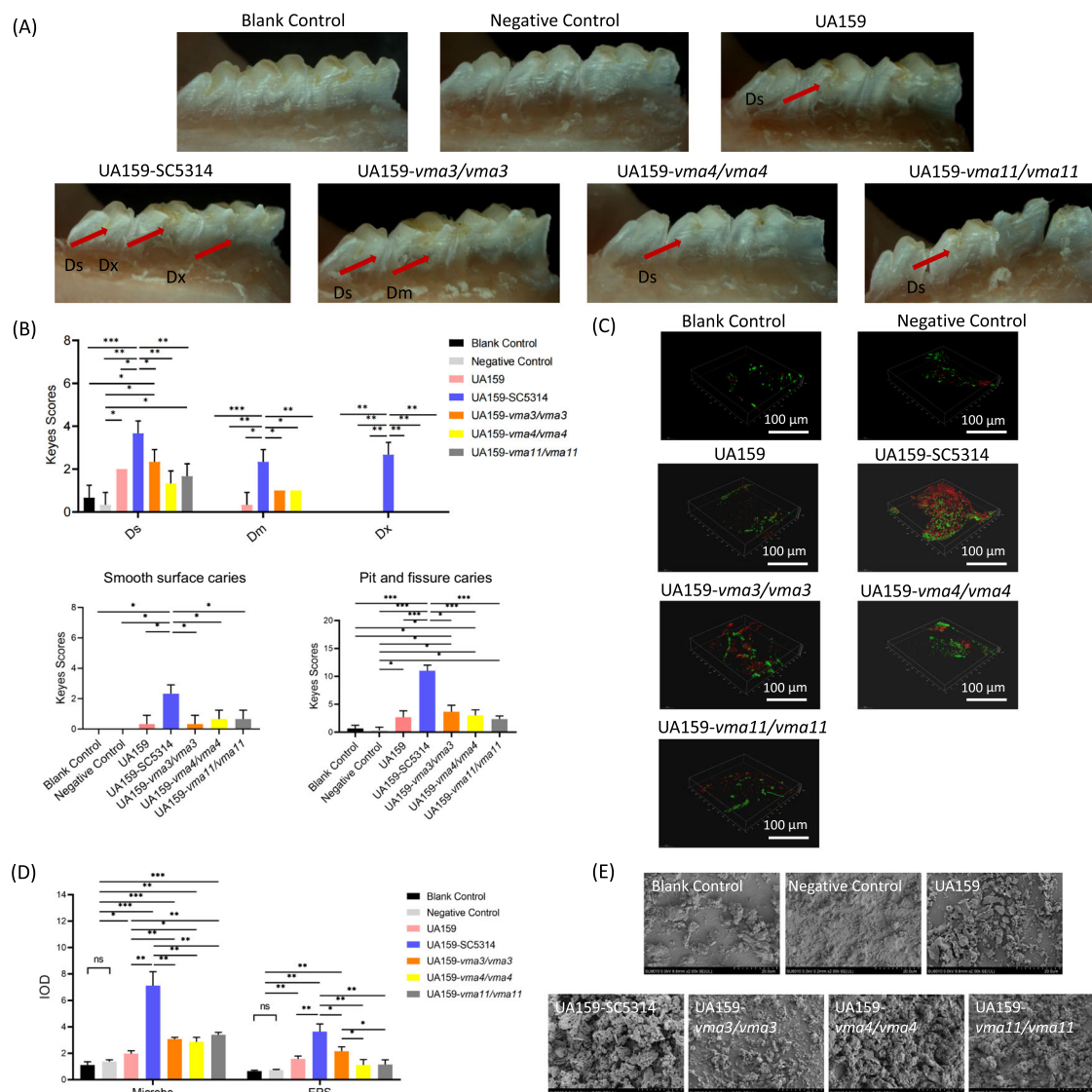


Fig. 7 | V-ATPase regulates cariogenicity of *C. albicans*-*S. mutans* biofilm in vivo. A Stereoscopic observation of caries. **B** Keyes score of caries at different sites. **C** Structure of dental plaque under CLSM. **D** Quantitative analysis of microbes and EPS in dental plaque. **E** Morphology of dental plaque under SEM.

homologous protein in human body, showing application potential as an anti-biofilm target. Therefore, we constructed *VMA3*, *VMA4*, and *VMA11* gene knockout mutants to further study the regulating effects of V-ATPase on the growth characteristics of *C. albicans* and the cariogenicity of *C. albicans*-*S. mutans* biofilm and its mechanisms.

VMA3, *VMA4*, and *VMA11* knockout mutants showed significant inhibition in growth and hyphal formation, and destruction of cell wall integrity. These results were consistent with previous studies, which verified the important role of V-ATPase in the growth and morphology of *C. albicans*^{22–27}. *C. albicans* mostly grows in a yeast form in acidic environment (pH < 6.5), and when exposed to neutral or alkaline environment (pH > 6.5), it shifts to a hyphal pathogenic form³⁵. The pH of human oral mucosa and saliva is 6.0 to 7.4, so *C. albicans* can be induced to hyphal form under appropriate conditions, making it easier to adhere to the tooth surface, interact with bacteria, and form dental plaque. In this study, *VMA3*, *VMA4*, and *VMA11* knockout mutants showed poor tolerance to alkaline environment, which may influence the colonization and hyphal development of *C. albicans* in the oral cavity, and further affect the adhesion and biofilm formation.

Dental plaque is an archetypical biofilm containing microbial cells and extracellular matrix. The extracellular matrix is composed of proteins and

polysaccharides, playing roles in the protection, nutrition and adhesion of microbial cells embedded in extracellular matrix. In this study, the ability of *VMA3*, *VMA4*, and *VMA11* knockout mutants to form *C. albicans*-*S. mutans* dual-species biofilm was significantly reduced, with decreased amounts of microbial cells and polysaccharides generation. *C. albicans* could not provide adhering sites to *S. mutans* by hyphal growth, resulting in loose biofilm structure. Consistently, in vivo experiments found that the coverage and thickness of dental plaque, the number of microbes and EPS, and the cariogenicity in rats in the group of *VMA3*, *VMA4*, and *VMA11* knockout mutants were significantly reduced compared with the positive control group. These results suggested that *C. albicans* could promote the adhesion and colonization of microbes on the tooth surface, and improve the cariogenicity of the biofilm. *VMA3*, *VMA4*, and *VMA11* were involved in these processes, indicating that *C. albicans* V-ATPase played an important role in regulating cariogenicity.

The cariogenicity of *S. mutans* is closely related to its ability of adhesion and EPS generation. The glucosyltransferases encoded by *gtfB*, *gtfC*, and *gtfD* are the key regulating factors for EPS generation^{36–38}, and the glucan binding proteins encoded by *gfbP* and *gfbC* mediate the adhesion of *S. mutans* to glucan^{39–41}. However, the dextranases encoded by *dexA* and *dexB* can hydrolyze glucan and destroy its binding sites, reducing the adhesion

ability of *S. mutans*^{42,43}. They also contribute to bacterial metabolism for energy storage and modifying glucans for their co-adhesion property^{42,44}. This study detected the gene expressions of *S. mutans* in the dual-species biofilms, showing that the expressions of *dexA* and *dexB* were significantly up-regulated after the knockout of *VMA3*, *VMA4*, and *VMA11*. By combining the results with the observation of biofilm structure and the detection of EPS, the decrease of EPS production in the mixed biofilm after the knockout of *VMA3*, *VMA4*, and *VMA11* was due to the reduced number of microbes and the increased expressions of the EPS degradation genes, which regulated glucose metabolism and structural features of the EPS.

The gene expressions of *C. albicans* in mixed biofilm were detected by transcriptome sequencing. The knockout of *VMA3*, *VMA4*, and *VMA11* interfered with the metabolism of various amino acids, fatty acids, and sugars, as well as the composition and function of ribosomes, mitochondria, and other organelles, leading to growth inhibition, damage, and death of fungal cells. Some genes involved in cell composition and meiosis were up-regulated, attempting to resist the internal and external stress. However, these genes failed to prevent the cell damage. Finally, the survival and metabolic activity of *C. albicans* were affected, leading to reduced abilities of *C. albicans*-*S. mutans* dual-species biofilm formation and polysaccharide utilization. Each stage of biofilm formation is regulated by related genes, in which adhesion and mycelia-related genes play an important role in the whole process. Agglutinin-like sequence (ALS) family genes are important adhesion related genes in *C. albicans*, encoding highly similar cell surface glycoproteins and playing a key role in adhesion, biofilm formation and primary invasion^{45,46}. Studies have shown that the glycosyltransferase GtfB secreted by *S. mutans* can bind to different sites on the surface of the cell wall of *C. albicans*, indicating that the fungal cell wall component ALS participates in the co-aggregation between *C. albicans* and *S. mutans*, and enhances the formation of biofilms of the two strains⁴⁷. Other studies have shown that the biofilm formation ability of ALS gene knockout mutants is significantly reduced. The fungal APSES protein family plays an important role in regulating morphological transformation, among which *Efg1* (enhanced filamentous growth 1) is considered to be the most important transcription factor of *C. albicans* morphological transformation, participating in the cAMP-PKA signaling pathway. Regulates the response of *C. albicans* to specific environmental stimuli and the formation of various specific cell phenotypes⁴⁸. The mycelia-specific gene *Ume6* is necessary for mycelia elongation and regulates the level and duration of mycelia-specific transcription. The mycelia-inducing conditions in the surrounding environment maintain mycelia elongation and sustainable development by stably activating the transcription factor *Ume6*⁴⁹. These results indicated that the mutant strains could significantly down-regulate the expression of these genes, thus affecting the whole process of biofilm formation from the early stage of biofilm development.

The c ring structure of V-ATPase V_0 domain is the main site of proton transport, which is mainly composed of eight c subunits, one c' subunit and one c'' subunit. Therefore, the c subunit encoding gene *VMA3* plays a crucial role in the activity of V-ATPase. In our study, the inhibition in cell growth and hyphal development of *C. albicans*, the reduced biomass and EPS generation of *C. albicans*-*S. mutans* biofilm, and the reduced cariogenicity of biofilms were more obvious in the *VMA3* deletion strain than those in the *VMA11* deletion strain. The *VMA4* encoded V_1 E is located at the periphery of the AB subunit hexamer, playing roles in the connection of V_1 and V_0 domains and the stability of V-ATPase, to ensure its correct assembly and function. Therefore, similar to *VMA3* deletion strain, the phenotype of *C. albicans* and *C. albicans*-*S. mutans* biofilm was also seriously affected after the knockout of *VMA4*. These results suggested that subunits of V-ATPase jointly maintain the integrity of its structure and function, and participate in regulating cariogenicity of biofilms.

In conclusion, we hypothesized that V-ATPase impacted the survival and virulence of *C. albicans* by regulating its ion homeostasis and hypha development, and then promoted the adhesion to *S. mutans* and the biofilm formation. With the changing biofilm microenvironment, the metabolic activities of microbial cells were regulated, including the EPS synthesis and

decomposition of *S. mutans*. As the result, the cariogenesis of biofilm was affected through glycoacid metabolic reprogramming.

As the *C. albicans*-*S. mutans* interaction play an important role in caries progression, it has great potential for the prevention and treatment of dental caries to reduce the cariogenicity of *C. albicans*-*S. mutans* biofilm by interfering with their interaction. Our study revealed the important regulatory effects of V-ATPase on the biofilm cariogenicity and its potential mechanisms through isolation and gene detection of *C. albicans* clinical strains, and experiments in vitro and in vivo based on the knockout of V-ATPase related genes. The results provided theoretical and experimental basis for seeking new strategy of caries ecological prevention and treatment targeting V-ATPase. Considering that the V_0 c' subunit encoded by *VMA11* had no homologous protein in human body, it may be an ideal target for V-ATPase inhibitors and antifungal drugs. More attempts can be made to interfere cross-kingdom biofilms by developing new molecular targeted compounds and nanomaterials.

Materials and methods

Strains and culture conditions

The wild type strains *C. albicans* SC5314 and *S. mutans* UA159 were commercially obtained from the American Type Culture Collection. The clinical strains of *C. albicans* were isolated from dental plaque using CHROMagar *Candida* medium and identified by PCR using the universal primers ITS1 (5'-CCGTAGGTGAACCTGCGG-3') and ITS4 (5'-TCCTCCGCTTA TTGATATGC-3'). The knockout mutants of *C. albicans* V-ATPase encoding genes *VMA3*, *VMA4*, and *VMA11* were constructed by fusion PCR strategies⁵⁰. Plasmids pSN52 and pSN40 were used for amplification of HIS1 and LEU2 markers, respectively. *C. albicans* genomic DNA was used for amplification of the 5'- and 3'- flanking fragments of the corresponding genes. The HIS1 and LEU2 markers flanked by *VMA3/4/11* 5'- and 3'- fragments were amplified with fusion PCR. The PCR products of the HIS1 and LEU2 markers were sequentially transformed into *C. albicans* WT, generating the *VMA3/4/11* gene deletion mutants. Primers used for PCR are listed in Table S1.

C. albicans strains were routinely cultured in YPD medium (20 g/L glucose, 20 g/L peptone, and 10 g/L yeast extract). Spider medium (10 g/L nutrient broth, 10 g/L mannitol, and 2.6207 g/L $K_2HPO_4 \cdot 3H_2O$) was used to assess hyphal formation. Brain-heart infusion (BHI) medium was used for routine growth of *S. mutans*. Solid medium was supplemented with 2% agar. *C. albicans* was incubated at 30 °C (for routine culture) or 37 °C (for hyphal induction) with shaking at 200 rpm aerobically, while *S. mutans* was incubated at 37 °C anaerobically (90% N_2 , 5% H_2 , 5% CO_2).

YNBB medium (0.67% YNB, 75 mM Na_2HPO_4 , 75 mM NaH_2PO_4 , 2.5 mM N-acetylglucosamine, 0.2% casamino acids, and 0.5% sucrose) was used for co-culture of *S. mutans* and *C. albicans*. Cells were harvested at mid-exponential phase by centrifugation. The density of *S. mutans* was adjusted to 1×10^6 colony-forming units (CFU)/mL and *C. albicans* to 1×10^4 cells/mL. Observations of dual-species biofilm were performed after 24 h incubation at 37 °C aerobically.

Clinical sample collection

Children aged between 3 and 12 were recruited from the Affiliated Hospital of Stomatology of Chongqing Medical University in Chongqing, China (ethical approval number: CQHS-IRB-2022-126). All of the participants received a comprehensive oral examination based on the standards of the World Health Organization "Oral health surveys: basic methods-5th ed"⁵¹. Children with dental caries (DMFT or dmft >0) were enrolled into the caries-active group (group CA), and healthy control individuals matched for age and gender to them were enrolled into the caries-free group (group CF). Subjects were excluded if they (i) had other bacterial or fungal infection oral disease, (ii) had oral mucosal disease, (iii) had gingivitis and periodontal disease, (iv) had systemic or congenital disease, (v) had received antibiotics within 3 months, or (vi) were undergoing orthodontic treatment. Parents or guardians of the participants were sufficiently informed about the aims of the research and voluntarily signed an informed consent according to the

recommendations of the Ethics Committee of Chongqing Medical University.

Participants were required to avoid eating, drinking, or tooth brushing 2 h before sample collection, and rinse their mouth with sterile saline. Supragingival plaque was scraped by a sterile Gracey curette, pooled into a sterile microcentrifuge tube on ice, and immediately stored at -80°C until further processing.

Growth curve assay

C. albicans cells of the WT strain and V-ATPase gene deletion mutants were incubated in YPD liquid medium overnight to stationary phase, and then transferred to fresh YPD liquid with an initial concentration of 5000 cells/mL. The cells were incubated at 30°C with shaking at 200 rpm. Cell densities were detected at different time points. Three independent repeats were performed.

Spot dilution assay

Overnight cultures of *C. albicans* in YPD liquid were tenfold serially diluted in distilled water at final concentrations ranging from 1×10^8 to 1×10^3 cells/mL. Subsequently, 2 μL of each dilution was spotted onto YPD plates with different pH values (pH 4, 5, 7.5, and 8). The growth conditions of the colonies were observed after 3 d of incubation at 37°C .

Morphological changes of *C. albicans* cells and *C. albicans*-*S. mutans* biofilm

The *C. albicans* cells harvested at mid-exponential phase and the *C. albicans*-*S. mutans* biofilms after 24 h incubation in YNBB were fixed with 2.5% (v/v) glutaraldehyde for 2 h at 4°C . The fixed samples were washed twice with phosphate buffered saline (PBS), dehydrated in a series of ethanol solutions (50, 75, and 90% for 10 min and then absolute alcohol for 10 min twice), and subsequently treated with a series of tert-Butanol solutions (50, 75, and 90% for 10 min and then absolute tert-Butanol for 10 min twice). The samples were freeze-dried, coated with a thin layer of gold-palladium, and observed under a scanning electron microscope (TM-3000, Hitachi, Japan).

Biofilm biomass assay by crystal violet staining

After being incubated in 96-well microtiter plate with YNBB as medium for 24 h, the biofilm was gently washed with PBS and stained with 0.1% crystal violet for 15 min. Then, the stained biofilm was washed again with PBS and the crystal violet was solubilize with 33% glacial acetic acid. The optical density was measured at 595 nm using a microplate reader (Cytation 3, BioTek, USA).

Exopolysaccharides assessment by anthrone method

The exopolysaccharides generation was assessed by anthrone method⁵². After being incubated in 24-well microtiter plate for 24 h, biofilms were harvested by scraping and vortexing in PBS buffer. The supernatant and sediment were harvested respectively by centrifugation (4000 rpm, for 15 min, at 4°C).

The supernatant containing water-soluble polysaccharides (WSG) was filtered through a 0.22 μm filter, and 20% trichloroacetic acid was added and the mixture was placed at 4°C for 2 h. The solution was centrifuged (4000 rpm) for 30 min at 4°C , and the supernatant was collected for WSG measurement.

The sediment was resuspended in 1 mL of 1 M NaOH and placed at 37°C for 3 h with shaking (200 rpm). After centrifugation (4000 rpm) for 15 min at 4°C , the supernatant was collected for WIG measurement.

Then, 600 μL of anthrone reagent was added to 200 μL of supernatant, and the mixtures were heated at 95°C for 10 min. The absorbance of each sample at 620 nm was monitored on a microplate reader. The standard curve was prepared with a dextran standard using various concentrations, and the corresponding polysaccharide concentration was calculated according to the standard curve.

Structural analysis of mixed biofilm by CLSM

The three-dimensional structures of the biofilms were observed under a confocal laser scanning microscope (CLSM) (TCS SP8, Leica, Germany).

To visualize EPS distribution, 1 μM Alexa Fluor 647 (Invitrogen, USA) were added into mix suspensions in confocal dishes before biofilm incubation. After incubation at 37°C for 24 h in the dark, the microbe cells were labeled with 2.5 μM SYTO9 (Invitrogen, USA).

To visualize the distribution of *C. albicans* and *S. mutans*, fluorescence in situ hybridization (FISH) was performed to label the two species with species-specific probes (Table S1)⁵³. The mix suspensions were incubated in confocal dishes at 37°C for 24 h in the dark for biofilm formation. After washing with PBS, 4% paraformaldehyde solution was added to fix the biofilms at 4°C for 10 h. The fixed biofilms were washed and dried at 46°C for 15 min, incubated in lysis buffer (0.1 M Tris-HCl, 50 mM EDTA, 30 g/L lysozyme) at 37°C for 20 min, dehydrated in a series of ethanol solutions (50, 80, and 96% for 3 min respectively), and dried at 46°C for 10 min. The FISH probes were dissolved and mixed with hybridization buffer (20 mM Tris-HCl, 0.9 M NaCl, 20% formamide, 0.01% SDS), and then added to the samples. After incubated at 46°C for 90 min in the dark, the samples were treated with washing buffer (20 mM Tris-HCl, 5 mM EDTA, 215 mM NaCl, 0.01% SDS) and incubated at 48°C for 15 min in the dark.

The biofilm samples were observed by CLSM with a 20 \times objective lens. The 3D images were reconstructed by Application Suite X (LAS X) software (Leica, Germany), and quantitative analysis of fluorescence was performed using ImageJ.

Expression analysis using qRT-PCR

C. albicans cells were harvested at mid-exponential phase by centrifugation. Biofilms were harvested by scraping after incubation in 6-well microtiter plate with YNBB as medium for 24 h. Total RNA was extracted using TRIzol reagent (Thermo Fisher Scientific, USA) according to manufacturer's instructions, and cDNA was prepared using RevertAid Reverse Transcriptase (Thermo Fisher Scientific, USA). Quantitative reverse real-time PCR (qRT-PCR) was performed in a Bio-Rad CFX96 real-time PCR detection system using SYBR Green qPCR mix (TOYOBO, Japan). The expression levels of each experimental sample were normalized to those of *ACT1* (for *C. albicans*) or *gyrA* (for *S. mutans*). Primers used in this analysis are listed in Table S1.

RNA-Seq analysis

Biofilms were harvested by scraping after incubation in 6-well microtiter plate with YNBB as medium for 24 h, and total RNA was extracted using TRIzol reagent. The RNA concentration was assessed by Nanodrop 2000 (Thermo Scientific, Wilmington, USA) and RNA quality was determined by 1% agarose gel electrophoresis. RNA-seq transcriptome library was prepared using TruSeqTM RNA sample preparation Kit (Illumina, San Diego, CA), and the library products were sequenced using an Illumina HiSeq Xten. The reads were separately aligned to reference genome (*C. albicans* SC5314) for analyses of differential expression and functional enrichment. The raw reads were deposited into the NCBI Sequence Read Archive (SRA) database (Accession Number: SRP488423).

To identify DEGs (differential expression genes) between different samples, the expression level of each transcript was calculated according to the transcripts per million reads (TPM) method. RSEM (<http://deweylab.biostat.wisc.edu/rsem/>)⁵⁴ was used to quantify gene abundances. Differential expression analysis was performed using DESeq2⁵⁵ with $\text{FDR} < 0.05$ & $|\log_2\text{FC}| \geq 1$ was considered to be significantly DEGs. The GO functional enrichment and KEGG pathway analysis were carried out by Goatools (<https://github.com/tanghaibao/Goatools>) and KOBAS (<http://kobas.cbi.pku.edu.cn/home.do>)⁵⁶ to identify GO terms and metabolic pathways DEGs significantly enriched in.

Cariogenicity of biofilms in vivo

Sprague-Dawley (SD) rats were used to investigate the effect of V-ATPase on the cariogenicity of dual-species biofilms in vivo. This study was approved by the Ethics Committee of Chongqing Medical University

(ethical approval number: CQHS-IRB-2022-066). SD rats (male, aged 4 weeks) were randomly divided into 7 groups ($n = 5$ per group), including (i) blank control, (ii) negative control (YNBB medium), (iii) *S. mutans* WT, (iv) *C. albicans* WT- *S. mutans* WT, (v) *C. albicans vma3/vma3-* *S. mutans* WT, (vi) *C. albicans vma4/vma4-* *S. mutans* WT, and (vii) *C. albicans vma11/vma11-* *S. mutans* WT.

C. albicans and *S. mutans* cells were harvested at mid-exponential phase and resuspended in YNBB medium with the concentration of *S. mutans* adjusted to 1×10^9 CFU/mL and *C. albicans* to 1×10^7 cells/mL. Then 200 μ L suspensions were orally infected to the mandibular molar area of rats using a cotton ball, daily for 10 days. All rats received cariogenic Diet 2000 and drinking water containing 5% sucrose, and animals were sacrificed under inhalation anesthesia 4 weeks after initial injection.

The smooth surface caries and sulcal caries on the molars were assessed by Keyes' procedure⁵⁷. The three-dimensional structure and the surface morphology of dental plaque biofilm were observed by CLSM and SEM, respectively.

Statistical analysis

Three independent experiments were performed for all in vitro analyses, and five parallels were set for each group in studies in vivo. The quantitative results are presented as mean \pm standard deviation. Statistical analyses were carried out using GraphPad Prism software (version 8.0, GraphPad, USA). After test for homogeneity of variance, one-way ANOVA and Dunnett's *t* test were performed to compare differences between multiple groups. Detection rates of *C. albicans* in dental plaque from caries-active and caries-free children were analyzed with chi-squared test. The expressions of V-ATPase related genes in clinical isolated strains were analyzed with student's *t*-test. Differences were considered statistically significant if $p < 0.05$.

Data availability

All data supporting the findings of this study are available within the paper and its Supplementary Information.

Code availability

The underlying code for this study is not publicly available but maybe made available to qualified researchers on reasonable request from the corresponding author.

Received: 27 March 2024; Accepted: 22 January 2025;

Published online: 08 March 2025

References

- Pitts, N. B. et al. Dental caries. *Nat. Rev. Dis. Primers* **3**, 17030 (2017).
- Hugo, F. N., Kassebaum, N. J., Marcenes, W. & Bernabé, E. Role of dentistry in global health: challenges and research priorities. *J. Dental Res.* **100**, 681–685 (2021).
- Collaborators, G.D.a.I.I.a.P. Global, regional, and national incidence, prevalence, and years lived with disability for 354 diseases and injuries for 195 countries and territories, 1990–2017: a systematic analysis for the Global Burden of Disease Study 2017. *Lancet* **392**, 1789–1858 (2018).
- Bernabé, E. et al. Global, regional, and national levels and trends in burden of oral conditions from 1990 to 2017: a systematic analysis for the global burden of disease 2017 Study. *J. Dental Res.* **99**, 362–373 (2020).
- Lamont, R. J., Koo, H. & Hajishengallis, G. The oral microbiota: dynamic communities and host interactions. *Nat. Rev. Microbiol.* **16**, 745–759 (2018).
- Verma, D., Garg, P. K. & Dubey, A. K. Insights into the human oral microbiome. *Archiv. Microbiol.* **200**, 525–540 (2018).
- Lemos, J. A. et al. The Biology of *S. mutans*. *Microbiol. Spectrum* **7**, <https://doi.org/10.1128/microbiolspec.GPP3-0051-2018> (2019).
- Lin, Y., Chen, J., Zhou, X. & Li, Y. Inhibition of *S. mutans* biofilm formation by strategies targeting the metabolism of exopolysaccharides. *Crit. Rev. Microbiol.* **47**, 667–677 (2021).
- Chin, V. K., Lee, T. Y., Rusliza, B. & Chong, P. P. Dissecting *C. albicans* Infection from the Perspective of *C. albicans* Virulence and omics approaches on host-pathogen interaction: a review. *Int. J. Mol. Sci.* **17**, 1643 (2016).
- Lohse, M. B., Gulati, M., Johnson, A. D. & Nobile, C. J. Development and regulation of single- and multi-species *C. albicans* biofilms. *Nat. Rev. Microbiol.* **16**, 19–31 (2018).
- Ghannoum, M. A. et al. Characterization of the oral fungal microbiome (mycobiome) in healthy individuals. *PLoS Pathog.* **6**, e1000713 (2010).
- Lueyar, T. K., Karygianni, L., Attin, T. & Thurnheer, T. Dynamic interactions between *C. albicans* and different streptococcal species in a multispecies oral biofilm. *MicrobiologyOpen* **12**, e1381 (2023).
- He, J. et al. RNA-Seq reveals enhanced sugar metabolism in *S. mutans* Co-cultured with *C. albicans* within mixed-species biofilms. *Front. Microbiol.* **8**, 1036 (2017).
- Falsetta, M. L. et al. Symbiotic relationship between *S. mutans* and *C. albicans* synergizes virulence of plaque biofilms in vivo. *Infection Immunity* **82**, 1968–1981 (2014).
- Sztajer, H. et al. Cross-feeding and interkingdom communication in dual-species biofilms of *S. mutans* and *C. albicans*. *ISME J.* **8**, 2256–2271 (2014).
- Hwang, G. et al. *C. albicans* mannans mediate *S. mutans* exoenzyme GtfB binding to modulate cross-kingdom biofilm development in vivo. *PLoS Pathog.* **13**, e1006407 (2017).
- Xiao, J. et al. *C. albicans* and early childhood caries: a systematic review and meta-analysis. *Caries Res.* **52**, 102–112 (2018).
- Lu, Y., Lin, Y., Li, M. & He, J. Roles of *S. mutans*-*C. albicans* interaction in early childhood caries: a literature review. *Front. Cell. Infection Microbiol.* **13**, 1151532 (2023).
- Brailsford, S. R. et al. The predominant aciduric microflora of root-caries lesions. *J. Dental Res.* **80**, 1828–1833 (2001).
- Lv, Q., Yan, L. & Jiang, Y. The importance of vacuolar ion homeostasis and trafficking in hyphal development and virulence in *C. albicans*. *Front. Microbiol.* **12**, 779176 (2021).
- Vasanthakumar, T. & Rubinstein, J. L. Structure and Roles of V-type ATPases. *Trends Biochem. Sci.* **45**, 295–307 (2020).
- Rane, H. S. et al. The contribution of *C. albicans* vacuolar ATPase subunit V₁B, encoded by *VMA2*, to stress response, autophagy, and virulence is independent of environmental pH. *Eukaryotic Cell* **13**, 1207–1221 (2014).
- Rane, H. S. et al. *C. albicans* *VMA3* is necessary for V-ATPase assembly and function and contributes to secretion and filamentation. *Eukaryotic cell* **12**, 1369–1382 (2013).
- Poltermann, S. et al. The putative vacuolar ATPase subunit Vma7p of *C. albicans* is involved in vacuole acidification, hyphal development and virulence. *Microbiology* **151**, 1645–1655 (2005).
- Mao, X. et al. Vacuole and Mitochondria Patch (vCLAMP) Protein Vam6 is involved in maintenance of mitochondrial and vacuolar functions under oxidative stress in *C. albicans*. *Antioxidants* **10**, 136 (2021).
- Kim, S. W. et al. Subunits of the vacuolar H⁺-ATPase complex, Vma4 and Vma10, are essential for virulence and represent potential drug targets in *C. albicans*. *Fungal Biol.* **123**, 709–722 (2019).
- Zhang, K. et al. Contribution of *VMA5* to vacuolar function, stress response, ion homeostasis and autophagy in *C. albicans*. *Future Microbiol.* **12**, 1147–1166 (2017).
- Qin, A. et al. V-ATPases in osteoclasts: structure, function and potential inhibitors of bone resorption. *Int. J. Biochem. Cell Biol.* **44**, 1422–1435 (2012).
- Breton, S. & Brown, D. Regulation of luminal acidification by the V-ATPase. *Physiology* **28**, 318–329 (2013).
- Chen, X. et al. Microbial etiology and prevention of dental caries: exploiting natural products to inhibit cariogenic biofilms. *Pathogens* **9**, 569 (2020).

31. Li, Y., Huang, S., Du, J., Wu, M. & Huang, X. Current and prospective therapeutic strategies: tackling *C. albicans* and *S. mutans* cross-kingdom biofilm. *Front. Cell. Infection Microbiol.* **13**, 1106231 (2023).
32. Duangthip, D. & Duangthip, D. Early childhood caries and *C. albicans*. *Evid. Based Dent.* **19**, 100–101 (2018).
33. Teng, F. et al. Prediction of early childhood caries via spatial-temporal variations of oral microbiota. *Cell Host Microbe* **18**, 296–306 (2015).
34. Zhang, Y. & Rao, R. The V-ATPase as a target for antifungal drugs. *Curr. Protein Peptide Sci.* **13**, 134–140 (2012).
35. Pan, L. et al. Phenotypic transitions and their regulatory mechanisms in the human fungal pathogen *C. albicans*. *Chin. J. Cell Biol.* **38**, 1049–1059 (2016).
36. Zhang, Q., Ma, Q., Wang, Y., Wu, H. & Zou, J. Molecular mechanisms of inhibiting glucosyltransferases for biofilm formation in *S. mutans*. *Int. J. Oral Sci.* **13**, 30 (2021).
37. Terao, Y., Isoda, R., Murakami, J., Hamada, S. & Kawabata, S. Molecular and biological characterization of gtf regulation-associated genes in *S. mutans*. *Oral Microbiol. Immunol.* **24**, 211–217 (2009).
38. Wang, R. et al. Nanoscale adhesion forces of glucosyltransferase B and C genes regulated Streptococcal mutans probed by AFM. *Mol. Oral Microbiol.* **35**, 49–55 (2020).
39. Lynch, D. J. et al. Cariogenicity of *S. mutans* glucan-binding protein deletion mutants. *Oral Health Dental Manag.* **12**, 191–199 (2013).
40. Matsumoto-Nakano, M., Fujita, K. & Ooshima, T. Comparison of glucan-binding proteins in cariogenicity of *S. mutans*. *Oral Microbiol. Immunol.* **22**, 30–35 (2007).
41. Matsumura, M. et al. The role of glucan-binding proteins in the cariogenicity of *S. mutans*. *Microbiol. Immunol.* **47**, 213–215 (2003).
42. Yang, Y. et al. Regulation of water-soluble glucan synthesis by the *S. mutans* dexA gene effects biofilm aggregation and cariogenic pathogenicity. *Mol. Oral Microbiol.* **34**, 51–63 (2019).
43. Colby, S. M., Whiting, G. C., Tao, L. & Russell, R. R. Insertional inactivation of the *S. mutans* dexA (dextranase) gene results in altered adherence and dextran catabolism. *Microbiology* **141**, 2929–2936 (1995).
44. Igarashi, T. et al. An essential amino acid residue for catalytic activity of the dextranase of *S. mutans*. *Oral Microbiol. Immunol.* **17**, 193–196 (2002).
45. Chen, H. F. et al. Role of SFP1 in the Regulation of *C. albicans* biofilm formation. *PLoS ONE* **10**, e0129903 (2015).
46. Hoyer, L. L. et al. *C. albicans* Agglutinin-Like Sequence (Als) Family Vignettes: a review of als protein structure and function. *Front. Microbiol.* **7**, 280 (2016).
47. Gregoire, S. et al. Role of glucosyltransferase B in interactions of *C. albicans* with *S. mutans* and with an experimental pellicle on hydroxyapatite surfaces. *Appl. Environ. Microbiol.* **77**, 6357–6367 (2011).
48. Doedt, T. et al. APSES proteins regulate morphogenesis and metabolism in *C. albicans*. *Mol. Biol. Cell* **15**, 3167–3180 (2004).
49. Lu, Y. et al. CO (2) Signaling through the Ptc2-Ssn3 axis governs sustained hyphal development of *C. albicans* by reducing Ume6 phosphorylation and degradation. *mBio* **10**, e02320–18 (2019).
50. Noble, S. M. & Johnson, A. D. Strains and strategies for large-scale gene deletion studies of the diploid human fungal pathogen *C. albicans*. *Eukaryotic cell* **4**, 298–309 (2005).
51. Organization, W. H. Oral health surveys: basic methods-5th ed. Geneva (Switzerland): World Health Organization (2013).
52. Lei, L. et al. Modulation of biofilm exopolysaccharides by the *S. mutans* vicX Gene. *Front. Microbiol.* **6**, 1432 (2015).
53. Klug, B. et al. Oral biofilm analysis of palatal expanders by fluorescence in-situ hybridization and confocal laser scanning microscopy. *J. Visualized Exp. JoVE* **20**, 2967 (2011).
54. Li, B. & Dewey, C. N. RSEM: accurate transcript quantification from RNA-Seq data with or without a reference genome. *BMC Bioinform.* **12**, 323 (2011).
55. Love, M. I., Huber, W. & Anders, S. Moderated estimation of fold change and dispersion for RNA-seq data with DESeq2. *Genome Biol.* **15**, 550 (2014).
56. Xie, C. et al. KOBAS 2.0: a web server for annotation and identification of enriched pathways and diseases. *Nucleic Acids Res.* **39**, W316–W322 (2011).
57. Keyes, P. H. Dental caries in the molar teeth of rats. I. Distribution of lesions induced by high-carbohydrate low-fat diets. *J. Dental Res.* **37**, 1077–1087 (1958).

Acknowledgements

This work was supported by the National Natural Science Foundation of China (NO. 32270888, 82301055, 32170194 and 32370202), Chongqing Natural Science Foundation Innovation and Development Joint Fund (Municipal Education Commission) Project (NO. CSTB2022NSCQ-LZX0039), Program for Youth Innovation in Future Medicine of Chongqing Medical University (NO. W0060), Program for Top talent Distinguished Progressor from Chongqing Medical University (NO. [2021]215), the China Postdoctoral Science Foundation (NO. 2023M730439), and the Chongqing Postdoctoral Science Foundation (NO. CSTB2023NSCQ-BHX0081).

Author contributions

Qian Jiang and Mengmeng Xu: Conceptualization, Resources, Methodology, Writing – original draft, Writing – review & editing. Hong Chen: Methodology. Yao Zhang: Investigation, Data curation. Yuting Sun: Methodology. Li Tao: Investigation, Conceptualization, Supervision, Funding acquisition. Zheng Wang: Conceptualization, Supervision, Funding acquisition. Deqin Yang: Conceptualization, Writing – review & editing, Supervision, Funding acquisition, Project administration.

Competing interests

The authors declare no competing interests.

Additional information

Supplementary information The online version contains supplementary material available at <https://doi.org/10.1038/s41522-025-00660-7>.

Correspondence and requests for materials should be addressed to Li Tao, Zheng Wang or Deqin Yang.

Reprints and permissions information is available at <http://www.nature.com/reprints>

Publisher's note Springer Nature remains neutral with regard to jurisdictional claims in published maps and institutional affiliations.

Open Access This article is licensed under a Creative Commons Attribution-NonCommercial-NoDerivatives 4.0 International License, which permits any non-commercial use, sharing, distribution and reproduction in any medium or format, as long as you give appropriate credit to the original author(s) and the source, provide a link to the Creative Commons licence, and indicate if you modified the licensed material. You do not have permission under this licence to share adapted material derived from this article or parts of it. The images or other third party material in this article are included in the article's Creative Commons licence, unless indicated otherwise in a credit line to the material. If material is not included in the article's Creative Commons licence and your intended use is not permitted by statutory regulation or exceeds the permitted use, you will need to obtain permission directly from the copyright holder. To view a copy of this licence, visit <http://creativecommons.org/licenses/by-nc-nd/4.0/>.

© The Author(s) 2025